Published in Journal of Crystal Growth 311, issue 8, 2490-2495, 2009
which should be used for any reference to this work

Evidence for an organic origin of pedogenic calcitic nanofibres

Guillaume Cailleau [a], Massoud Dadras [b], Sousan Abolhassani-Dadras [c], Olivier Braissant [d], Eric P. Verrecchia [a,*]

[a] *Institut de Géologie et de Paléontologie, Université de Lausanne, Antropole, 1015 Lausanne, Switzerland*
[b] *Service de microscopie et nanoscopie, Université de Neuchâtel, Rue Jaquet-Droz 1, 2007 Neuchâtel Switzerland*
[c] *Paul Scherrer Institute, 5232 Villigen PSI, Switzerland*
[d] *Universität Basel, Biozentrum-Pharmazentrum, Klingelbergstrasse 50-70, CH-4012 Basel, Switzerland*

A B S T R A C T

Calcium carbonate nanofibres are found in numerous terrestrial environments, often associated with needle fibre calcite. This study attempts to mimic the natural system and generate comparable crystalline structures. A comparison of natural and synthesized nanofibre structures, using HRTEM as well as electron energy loss spectroscopy (EELS) and electron spectroscopic imaging (ESI), has demonstrated that this type of nanocrystal can result from precipitation on organic templates, most likely cellulose nanofibres. This study emphasizes the fundamental role of organic templates in the precipitation of calcium carbonate in vadose environments, even at the nanoscale.

Keywords: Biomaterials, Biocrystallization, Nanostructures, Natural crystal growth, Minerals

1. Introduction

In numerous terrestrial environments where carbonate precipitation occurs, a peculiar kind of nanofibre is often observed [1–5]. Their origin remains unclear. They are found in cave deposits, such as moonmilk [6], in which they constitute a large part of the total dry volume. They have also been observed in soils from Africa [7] and the French Jura Mountains. Unduly called "fibre calcite crystals" in reference to needle fibre calcite (NFC) [8], these rods, with their diameters never exceeding 30 nm, are drastically different from NFC. The purpose of this paper is to challenge the assumption that organic nanofibres could be at the origin of crystalline nanofibres, based on the existence of calcite pseudomorphoses of macroscopic cellulose fibres [7], and the observation of decaying organic filaments showing nanofibre structures. In this study, the term "nanofibres" denotes organic material that can undergo mineralization. A crystalline nanofibre is simply referred to as a nanofibre.

*Corresponding author.
E-mail address: eric.verrecchia@unil.ch (.P. Verrecchia).

2. Materials and methods

2.1. Materials

Two categories of nanofibres were studied: (i) natural and (ii) synthetized samples. Natural samples have been collected at three different sites: (i) in Ivory Coast, where these nanofibres have been sampled in soils around the Iroko tree (*Milicia excelsa*) where calcium carbonate accumulation occurs [7], (ii) in the Alps, from the Cornettes de Bises cave (Valais, Switzerland) where moonmilk has been sampled close to the entrance of the cave as a 20 cm thick cave wall coating, and (iii) in a French Jura Mountains soil (Loue Valley).

To reproduce crystalline nanofibres, three kinds of commercial organic fibres have been tested: cellulose, chitin, and chitosan. These organic fibres are commonly found in plants and fungal tissues. A weakly undersaturated calcium carbonate solution (prepared with pure analytical reagents: pure water, Merck calcium carbonate) has been mixed with these organic fibres.

2.2. Sample preparation

Sample preparation has been different for each observation technique. For low-temperature scanning electron microscopy

(LTSEM) observations, the samples were prepared by quenching in liquid nitrogen cooled at −205 °C. The cooled sample was broken under the vacuum of 10^{-4} mbar. To remove the extra water present in the microstructure and to reveal the sample structure itself, it was sublimated at −95 °C and 10^{-4} mbar for 10 min. About a 10 nm Pt coating was deposited on the sample to improve the surface conductivity for imaging. LTSEM observations were carried out at −120 °C. In preparation for transmission electron microscopy (TEM), about 30 μL of the sample was deposited on either a TEM carbon-coated grid, and slowly dried at ambient temperature in a sterile dust-free environment for synthesized samples, or on the 300 mesh carbon film copper grid in the absence of any solvent for natural samples. Synthetized samples were produced in series and analysed 3 weeks to 1 month later.

2.3. Instrumentation

Observations of samples have been performed using a Phillips ESEM-FEG XL30 equipped with an EDAX energy-dispersive spectrometer (EDS). The microscope was also equipped with a Gatan Alto 2500, permitting low-temperature sample preparation and LTSEM observations. TEM observations were carried out using a Phillips CM-200 transmission electron microscope with an acceleration voltage of 200 kV equipped with a Gatan CCD camera and EDAX EDS microprobe. Electron energy loss spectroscopy (EELS) and electron spectroscopic imaging (ESI) analyses have been performed using a Zeiss CM902 (to permit element mapping).

3. Experimental results

3.1. SEM observation of natural samples

The observation of moonmilk by LTSEM (Fig. 1A) shows that it is composed of a dense mesh of mineral nanofibres arranged mostly randomly. The diameter of the mineral nanofibres is about 30 nm and their length 1.6 μm. Also present is a needle-like calcite crystal, with a diameter of about 2 μm. In some areas, the nanofibres show a directionally organized matrix of crossed nanofibres oriented mainly in two preferential directions (Fig. 1B). EDS analyses performed on a dense mesh of nanofibres clearly show the presence of calcium. The sample etched by a solution of hydrochloric acid demonstrated that no nanofibres remain, except some microscopic organic filaments interpreted as actinomycetes, based on their size and shape. The presence of actinomycetes has already been documented in hypogean environments [9,10].

Associated with these nanofibres are numerous crystals of needle fibre calcite (NFC; arrow 1 Fig. 1C). It is interesting to note that some filaments identified as organic in origin can be the source of nanofibres due to decay processes (white arrow 2 Fig. 1C). In African soils (Fig. 1D), the general appearence of the sample is the same as moonmilk: randomly oriented mineral microfibres. The arrows in Fig. 1D indicate the mineral nanofibres showing some curvature, which confirms the flexibility of the original nanofibres, before mineralizing and becoming inflexible.

In addition, some nanofibres have also been observed associated with bundles of needle fibre calcite. This association has previously been noted in Ivory Coast soils [7] in the presence of biogenic carbonate as well as in calcretes [1,8].

3.2. TEM observations and microdiffraction of natural samples

Transmission electron microscope observations were carried out on samples from Ivory Coast. As observed with SEM, a lattice of crossed nanofibres are also visible with TEM (Fig. 2A). TEM observations allow the measurement of nanofibre diameters, which are between 19 to 30 nm. By tilting the sample around the longitudinal axis from +45° to −45°, some nanofibres are observed

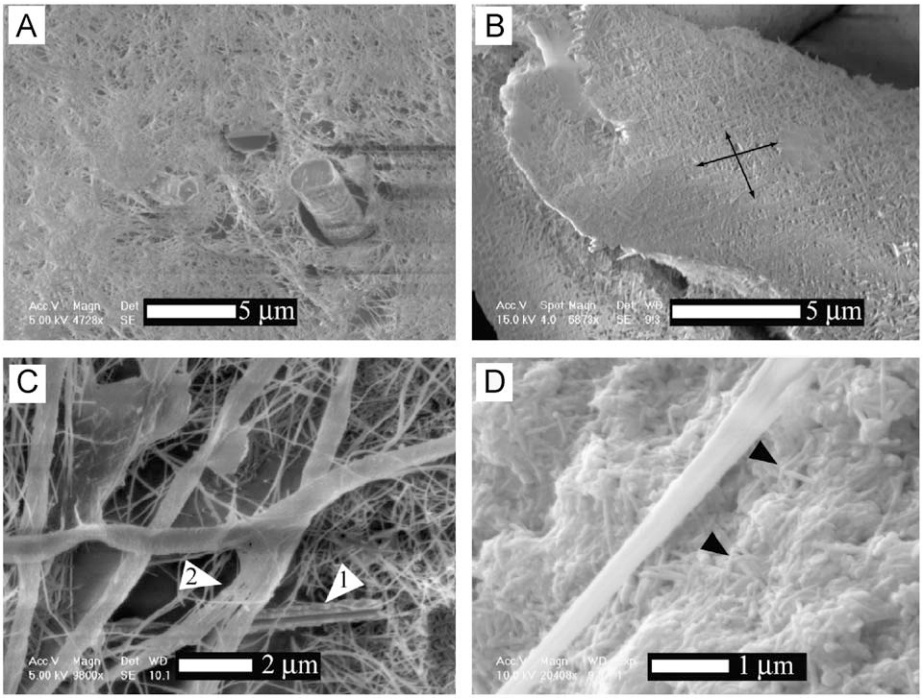

Fig. 1. (A–C) Low-temperature scanning electron microscope (LTSEM) images of moonmilk from the Cornettes de Bises cave (Valais, Switzerland). (A) High density of nanofibres in an unorganized mesh found in moonmilk. (B) Detail of an organic mesostructure showing a mesh of intertwined nanofibres mainly oriented in two directions. (C) Some organic filaments (streptomyscetes?) are found in cave moonmilk. Some of them seem to decay as nanofibres (arrow). (D) SEM image of a soil sample from Ivory Coast. Nanofibres with the same characteristic size as moonmilk are also observed. Note that some nanofibres (arrows) are bent in contact with underlying ones, indicating their flexibility.

to be undulating (at least in one plane; Fig. 2B) and some are straight (Fig. 2C). The contrast observed in nanofibres (Fig. 2B and C) could be related to a difference in internal and external structure. The internal dark area is surrounded by a brighter outline (Fig. 2B and C). This bright external layer has a thickness of 6.5–7.3 nm. Microdiffraction analyses of nanofibres demonstrate that most of them are monocrystalline in nature (Fig. 2C). The crystalline structure is difficult to determine as the nanofibres are very unstable under the focused beam. After only a few seconds of irradiation by the accelerated electrons, the crystalline structure of nanofibres is transformed, making it impossible to obtain more than one diffraction pattern of the original monocrystal for lattice parameter determination. HRTEM observations of the surface of nanofibres show the presence of 5–7 nm crystals (Fig. 2D). The presence of such fine features could be explained by the transformation of a monocrystal nanofibre to a nanocrystalline structure during observation and the damage introduced by the electron beam. As only one diffraction pattern is present for the whole nanofibre, this implies that it has a single crystalline structure.

In the TEM bright field (BF) and dark field (DF) (Fig. 3A and B) nanofibres from Ivory Coast appear to be quite straight and have a diameter of <10 nm with length of >1 μm. In conclusion, natural nanofibres are organized as a mesh, sometimes intertwining. They are up to 30 nm in diameter and up to 1.6 μm in length. Some of them seem to have an internal structure and their crystalline nature is emphasized by crystallographic pattern. Although they are calcitic in nature, they are different in size and structure [11] from the NFC with which they are often associated.

3.3. TEM observations and electron diffraction of synthesized samples

After experimental mineralization of three types of nanofibres with $CaCO_3$ enriched solutions, comparison between natural nanofibres and synthesized samples shows that cellulose nanofibres are the best match with the natural ones. Fig. 3C and D present the electron micrographs obtained by TEM in bright and dark fields. The difference in contrast between internal and external structures could be related to the difference in crystalline structures between these two parts of the crystal. The same variation observed in contrast in natural nanofibres is shown in Fig. 3A and B. It is concluded that this homology of structure makes the commercial nanofibres a proxy to the natural ones. Chitin and chitosan nanofibres are substantially different to natural ones in terms of size, dark and bright field responses. Consequently, they have not been chosen for further experiments. In conclusion, only cellulose has been compared to natural samples.

Microdiffraction has been performed on a synthesized nanofibre (the diffraction pattern is shown in Fig. 3E), indicating that the material is crystalline. HRTEM observation (Fig. 3F) also displays atomic planes, which seem to correspond to the outer layer observed in bright field or the double bright layer seen in dark field. In conclusion, synthesized nanofibres based on

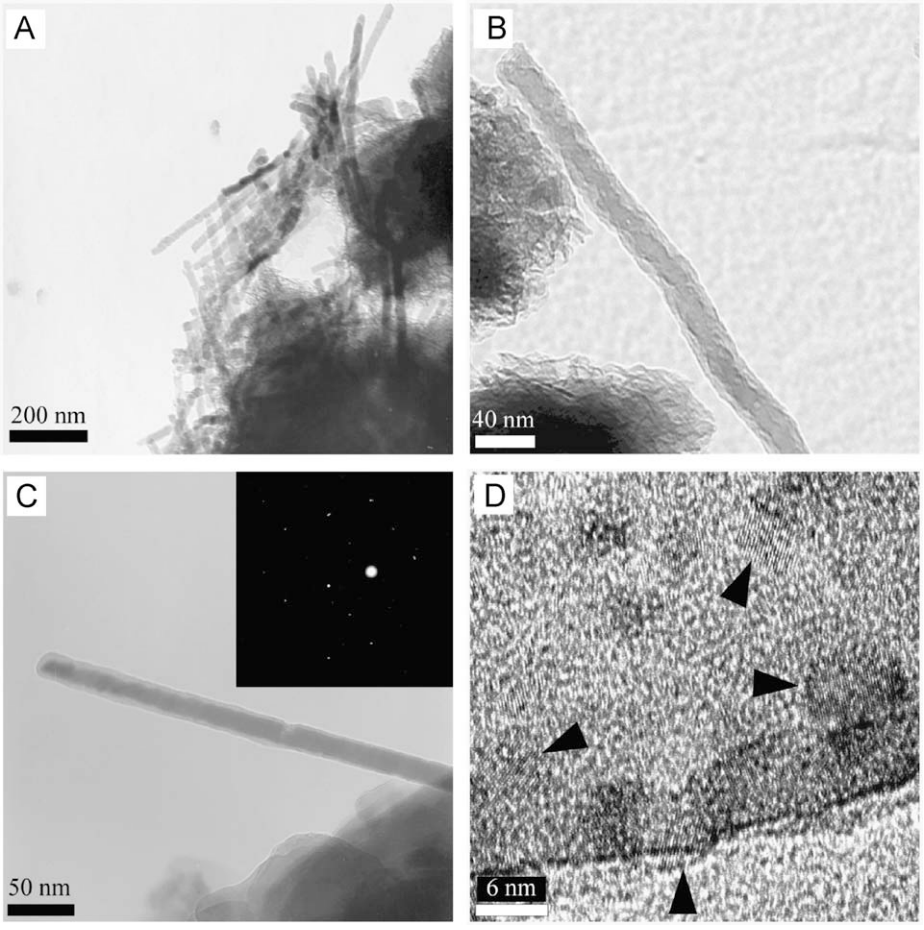

Fig. 2. Nanofibres found associated with secondary carbonates in an orthox soil (Ivory Coast). (A) TEM view of a nanofibre mesh. (B) Some rods have an undulating longitudinal void inside them. (C) Another example of a nanofibre. This feature has an internal structure. Top-right-hand corner of image: microdiffraction pattern of a nanofibre demonstrating its crystallographic nature. (D) HRTEM view of a nanofibre edge showing nanocrystals emphasized by the stacking of atomic planes (arrows).

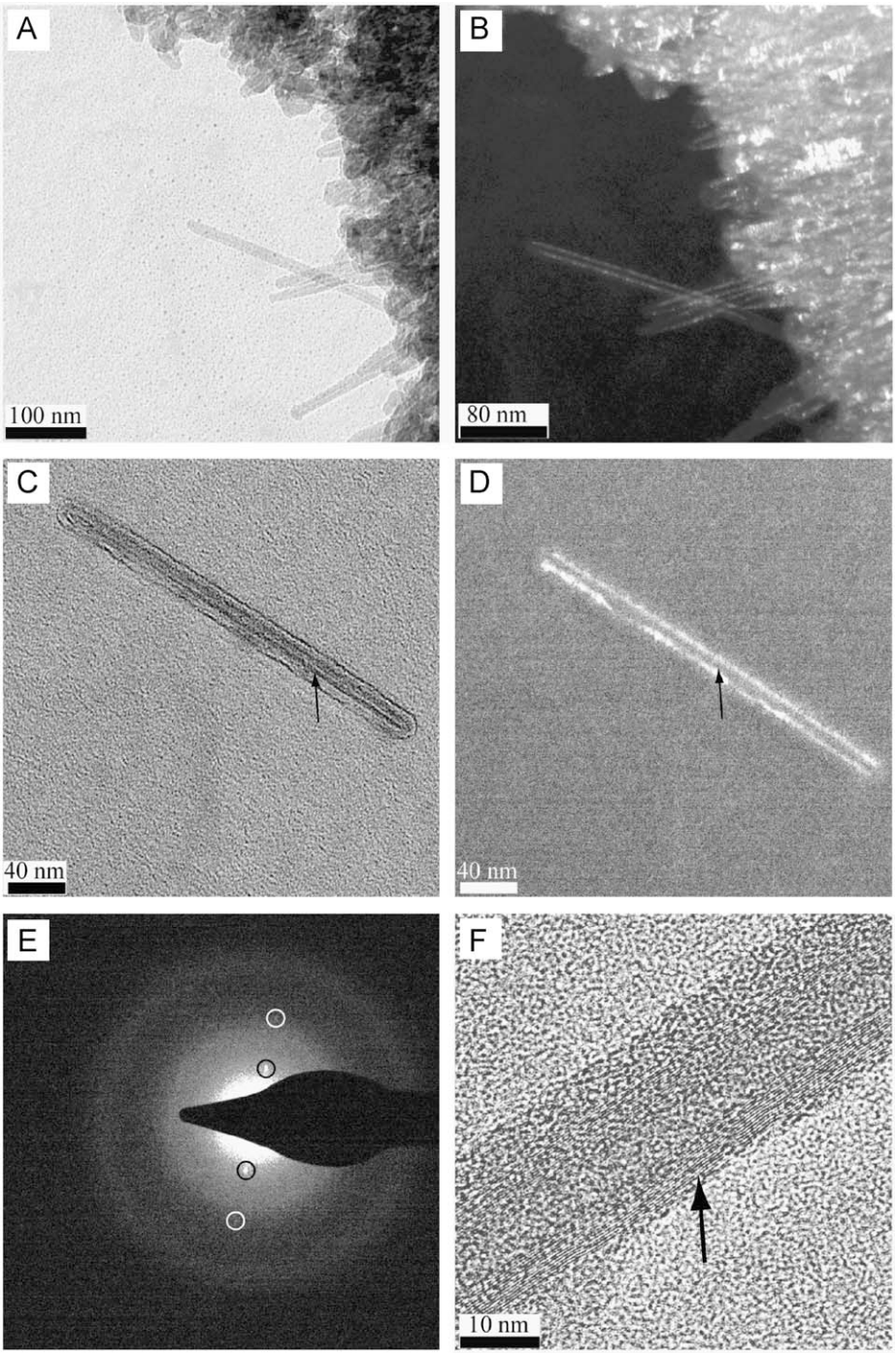

Fig. 3. (A–D) TEM images showing natural and synthesized nanofibres. (A and B) Natural nanofibres from orthox soils (Ivory Coast). These nanofibres have internal structures giving a typical pattern in bright and dark fields. (C and D) Synthesized nanofibre produced by adding 50 μl (5 times 10 μl) of a cellulose mixture to a solution 50% saturated in $CaCO_3$ on a TEM grid. Nanofibres are similar to natural ones shown in A and B. They show the same kind of internal structure in bright (C, arrow) and dark (D, arrow) fields as those shown in A and B. (E) Microdiffractogram of one of these nanofibres, demonstrating their crystallographic nature. (F) HRTEM image of a nanofibre produced during the experiment and showing well-organized atomic planes. Compare with Fig. 2F.

cellulose material show virtually the same structure as natural nanofibres, including differentiation between internal and double mineralized external layers.

3.4. EELS and ESI analyses of synthesized samples

Due to the very small size of the fibres and the limitation of the spatial resolution of EDS analysis in the absence of a STEM unit, EELS and ESI measurements have been performed on the fibres. To determine element composition, cellulose-based nanofibres have been first analysed using EELS (Fig. 4). Three peaks have been identified in the EELS spectrum. The first is a carbon peak corresponding to the carbon from the grid film, which is also present in the cellulose. After deconvolution, the peaks of potassium and calcium have also been obtained. These two elements have an overlapping spectrum. Therefore, after this first step, it was possible to select the energy windows for electron

spectroscopic imaging. Due to the different location of potassium and calcium, the two elements could be separated in the ESI maps (Fig. 5). As observed in Fig. 5C and D, the calcium signal was present only for the external structure of the fibres, whereas the potassium was present for the internal structure. These two elements could therefore be separated.

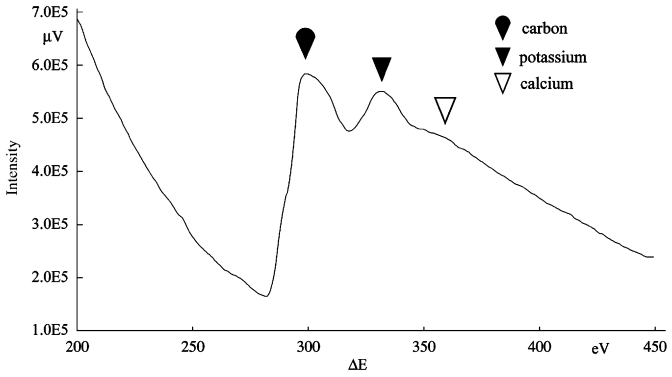

Fig. 4. An EELS spectrum of nanofibre pile produced during the experiment and showing three peaks interpreted as carbon, potassium and calcium. K and Ca peaks are theoretically overlapping and so, seem to be stacked to the C background spectrum. Peak deconvolution defines a range of energies exclusively related to Ca and excluding K.

4. Discussion

Nanofibres are often associated with NFC. Does this mean that their origins are related? In the literature, nanofibres are considered to be crystals precipitated as precursors to NFC in supersaturated solutions [6,12]. The main problem is that the structure of nanofibres is significantly different from that of NFC. A nanofibre is not an intermediate stage nor does it evolve into another form of habit: the only organized structure observed at a higher scale is a mesh with totally mineralized intertwined rods (also observed by Borsato et al. [6]). Therefore, it is reasonable to consider that their shape as well as their structure could be explained by a process other than a purely physico-chemical one. Organic nanofibres could act as a template for precipitation of calcium carbonate to form nanofibres. The comparison made between natural and synthesized samples (e.g. cellulose fibres) shows great similarities, especially regarding sizes and structures. The presence of decaying filaments, which exhibit an internal structure partly composed by fibres, and the texture observed using TEM, suggest that the mesh of natural fibres could be composed by cellulose.

Two points must be discussed: the diffraction of commercial cellulose after experimental treatment and HRTEM observations. It is known that cellulose can diffract [13]. Therefore, it is difficult to determine if it is cellulose or a calcium carbonate nucleation that has been detected during microdiffraction. Nevertheless, HRTEM observations show regular atomic planes all around the

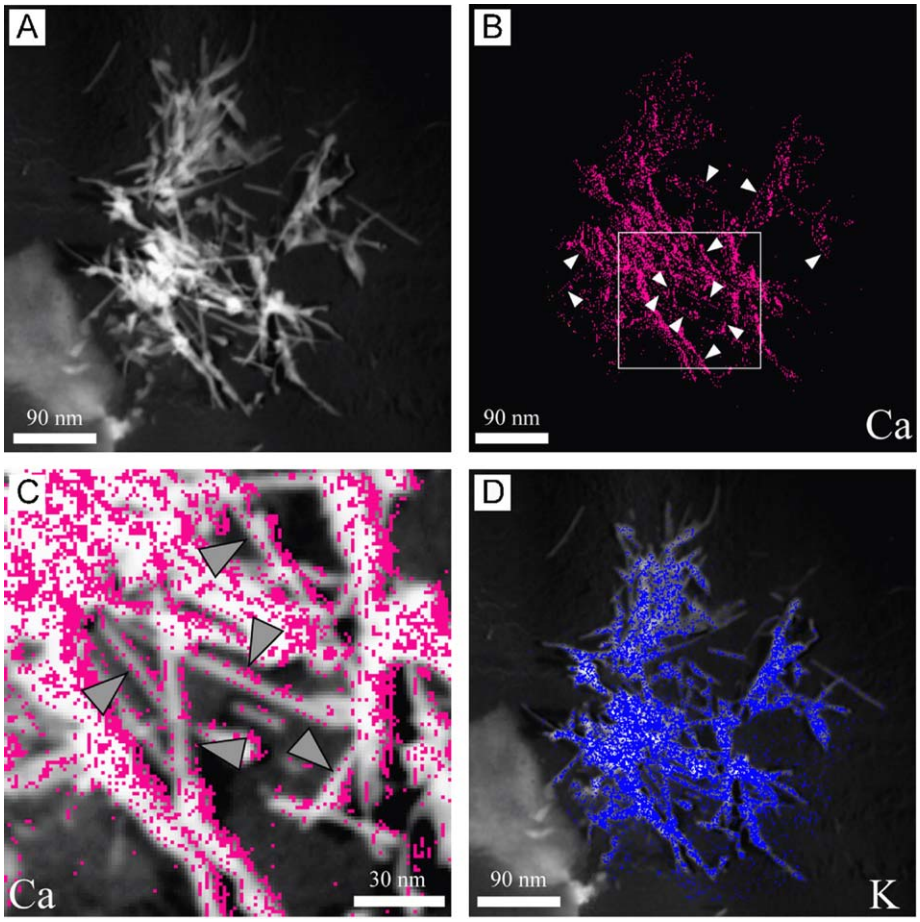

Fig. 5. (A) Inelastic scattering TEM image of a nanofibre pile from which an EELS spectrum is given in Fig. 4. (B) Ca mapping (fuchsia). Note that Ca is preferentially detected in nanofibre edges forming alignment of parallel points (arrows) according to the nanofibre shape. (C) Detail of the previous map showing Ca presence at the edge of nanofibres (arrows). (D) K mapping (blue color) superimposed on image (A) showing the different behaviours of K and Ca. These two elements are not correlated. (For interpretation of the references to color in this figure legend, the reader is referred to the web version of this article.)

nanofibre (Fig. 3F). This kind of regular structure can be interpreted as a lattice surrounding the cellulose fibre. Its nature is interpreted as a calcium carbonate coating, which is to be expected after the laboratory processing. The presence of insoluble sugar (in the synthetized conditions) in the fibre is unlikely. Moreover, as shown by Brooks et al. [14] and Ben Chekroun et al. [15], the weak diffraction pattern (Fig. 3E) could result from the low crystallinity of calcium carbonate. Is the calcium carbonate, detected on the nanofibre, purely crystalline, amorphous, or hydrated? To determine its nature, *in situ* analyses have to be performed. Unfortunately, the EDS method remains inappropriate.

Consequently, the nature of these crystalline features had to be tested using EELS and ESI methods. The EELS spectrum has shown the presence of two elements, i.e. calcium and potassium. Although the source of calcium is obvious (provided by the calcium carbonate solution), potassium cannot come from the experimental solution. Potassium is provided by the commercial cellulose. It is common in the industry to use potassium chemical compounds (e.g. potassium hydroxide) for pulp bleaching, explaining the presence of potassium. As the two elements have their peaks partly superimposed on the EELS spectrum, the edge-energies (CaL edge is at 346 eV, KL edge is at 294 eV) have been chosen to distinguish between the two elements using ESI (Fig. 5A). The two maps for calcium and potassium are different and are not superimposed (Fig. 5B, D). Potassium is detected for the whole nanofibre (Fig. 5B and D) whereas calcium is mainly mapped in the outer layer (Fig. 5B and C). The two maps obtained using the edge-energies are different, indicating that the energy boundaries are valid. The presence of calcium seems to exclude the hypothesis that regular atomic planes all around the nanofibre could be composed by sugar. Consequently, it can be concluded that these nanocrystals constitute a calcium carbonate coating precipitated during the experimental drying on the TEM grid.

The comparison of synthesized and natural nanofibres shows that they share many characteristics (size, some bright field and dark field observations, HRTEM observation of atomic planes). Calcite pseudomorphoses of cellulose macrofibres have already been observed [7]. This argument supports the hypothesis that cellulose nanofibres could also be pseudomorphosed by a calcitic solution. In conclusion, all natural nanofibres can be explained either by a simple coating of calcium carbonate or by a calcitic pseudomorphose of organic templates.

5. Conclusion

These investigations have shown a possible interpretation of the origin of calcitic nanofibres ubiquitously found in terrestrial carbonate environments. They suggest that these apparently originally flexible nanofibres (interpreted here as cellulose nanofibres) could be either the template for carbonate coating precipitation (which is common in soil organic matter), or be pseudomorphosed by the carbonate solution present in the soil environment. The existence of calcitic pseudomorphose of cellulose nanofibres is supported by observations of cellulose macrofibres, also pseudomorphosed by calcite. The existence of a natural calcitic coating on a lengthened support could be explained by experimental reproduction with cellulose nanofibres as shown by ESI. This study emphasizes the catalytic behavior of organic matter as a template for calcium carbonate precipitation in vadose environments at the nanoscale. It provides another hypothesis for nanofibre formation. These calcitic nanofibres can constitute one-third of cave moonmilk, emphasizing the impact of such a process in terrestrial calcium carbonate dynamics.

Acknowledgments

The authors wish to thank the centre of Electron Microscopy of the University of Lausanne for the use of their Zeiss CM902 microscope. The CSRS (Swiss Science Research Centre, Abidjan, Ivory Coast) provided field help. This study was supported by the Swiss National Science Foundation, Grant nos. 2153-065174.01 and 205320-101564.

References

[1] C. Loisy, E.P. Verrecchia, P. Dufour, Sediment. Geol. 126 (1999) 193.
[2] J.C. Cañaveras, S. Sanchez-Moral, V. Soler, C. Saiz-Jimenez, Geomicrobiol. J. 18 (2001) 223.
[3] D.E. Northup, K.H. Lavoie, Geomicrobiol. J. 18 (2001) 199.
[4] S. Sanchez-Moral, J.C. Cañaveras, L. Laiz, C. Saiz-Jimenez, J. Bedoya, L. Luque, Geomicrobiol. J. 20 (2003) 491.
[5] B. Bajnóczi, V. Kovács-Kis, Chem. Erde (2005)10.1016/j.chemer.2005.11.002.
[6] A. Borsato, S. Frisia, B. Jones, K. van der Borg, J. Sediment. Res. 70 (2000) 1179.
[7] G. Cailleau, O. Braissant, C. Dupraz, M. Aragno, E.P. Verrecchia, Catena 59 (2005) 1.
[8] N.P. James, J. Sediment. Petrol 42 (1972) 817.
[9] J.C. Cañaveras, S. Cuezva, S. Sanchez-Moral, J. Lario, L. Laiz, J.M. Gonzalez, C. Saiz-Jimenez, Naturwissenschaften 93 (2006) 27.
[10] I. Groth, C. Saiz-Jimenez, Geomicrobiol. J. 16 (1999) 1.
[11] E.P. Verrecchia, K.E. Verrecchia, J. Sediment. Res. 64 (1994) 650.
[12] B. Jones, C.F. Kahle, J. Sediment. Petrol. 63 (1993) 1018.
[13] M. Müller, C. Czihak, M. Burghammer, C. Riekel, J. Appl. Cryst. 33 (1998) 817.
[14] R. Brooks, L.M. Clark, E.F. Thurston, Phil. Trans. R. Soc. London 243 (1950) 145.
[15] K. Ben Chekroun, C. Rodríguez-Navarro, M.T. González-Muñoz, J.M. Arias, G. Cultrone, M. Rodríguez–Gallego, J. Sediment. Res. 74 (2004) 868.